Time Correlation Function Modeling of Third-Order SFVS of a Charged Surface/Water Interface.

ARTICLE *in* THE JOURNAL OF PHYSICAL CHEMISTRY B · NOVEMBER 2014

Impact Factor: 3.3 · DOI: 10.1021/jp509647w · Source: PubMed

2 AUTHORS:

Anthony J Green

University of South Florida

6 PUBLICATIONS **77** CITATIONS

SEE PROFILE

Brian Space

University of South Florida

91 PUBLICATIONS **1,947** CITATIONS

SEE PROFILE

THE JOURNAL OF PHYSICAL CHEMISTRY B

Article

pubs.acs.org/JPCB

Time Correlation Function Modeling of Third-Order Sum Frequency Vibrational Spectroscopy of a Charged Surface/Water Interface

Anthony J. Green and Brian Space*

Department of Chemistry, University of South Florida, Tampa, Florida 33620-5250, United States

ABSTRACT: Sum frequency vibrational spectroscopy (SFVS), a second-order optical process, is interface-specific in the dipole approximation [Perry, A.; Neipert, C.; Moore, P.; Space, B. *Chem. Rev.* **2006**, *106*, 1234−1258; Richmond, G. L. *Chem. Rev.* **2002**, *102*, 2693−2724; Byrnes, S. J.; Geissler, P. L.; Shen, Y. R. *Chem. Phys. Lett.* **2011**, *516*, 115−124]. At charged interfaces, the experimentally detected signal is a combination of enhanced second-order and static-field-induced third-order contributions due to the existence of a static field. Evidence of the importance/relative magnitude of this third-order contribution is seen in the literature [Ong, S.; Zhao, X.; Eisenthal, K. B. *Chem. Phys. Lett.* **1992**, *191*, 327−335; Zhao, X.; Ong, S.; Eisenthal, K. B. *Chem. Phys. Lett.* **1993**, *202*, 513−520; Shen, Y. R. *Appl. Phys. B: Laser Opt.* **1999**, *68*, 295−300], but a molecularly detailed approach to separately calculating the second- and third-order contributions is difficult to construct. Recent work presented a novel molecular dynamics (MD)-based theory that provides a direct means to calculate the third-order contributions to SFVS spectra at charged interfaces [Neipert, C.; Space, B. *J. Chem. Phys.* **2006**, *125*, 224706], and a hyperpolarizability model for water was developed as a prerequisite to practical implementation [Neipert, C.; Space, B. *Comput. Lett.* **2007**, *3*, 431−440]. Here, these methods are applied to a highly abstracted/idealized silica/water interface, and the results are compared to experimental data for water at a fused quartz surface. The results suggest that such spectra have some quite general spectral features.

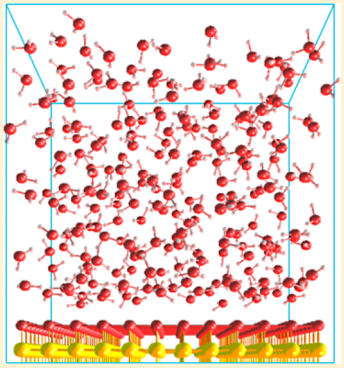

1. INTRODUCTION

Aqueous interfaces are abundant in the environment and vital to many chemical, biological, and atmospheric processes. Typically, these interfaces are not neat and contain charged species or charged solid surfaces, such as silica in its many forms. Naturally occurring silica/water interfaces are ubiquitous, and many important chemical processes occur in soil and atmospheric dust, where silicates are widespread.[1−6] A charged interface is created between water and silica by the presence of silanol groups (SiOH), which terminate silica and tend to ionize in water, especially as the pH is increased.[7,8] A relatively large static field is also produced by the undissociated silica surface due to large charge separation between the silicon, oxygen, and hydrogen atoms.[9,10]

In a typical sum frequency vibrational spectroscopy (SFVS) experiment, a signal is generated by combining visible and infrared laser pulses focused in time and space upon the interface to be studied. A major component of the resulting signal is a second-order response that requires anisotropic media according to the dipole approximation.[11−13] Interfaces inherently disrupt the symmetry due to the lack of an inversion center that gives rise to the interface specificity needed for a response. When the infrared laser frequency corresponds to a vibration at the interface, a resonant line shape is obtained with a characteristic shape that reflects both the structural and dynamical environment at the interface.[14−17] If a static field is present, the third-order susceptibility is probed in addition to the second-order susceptibility from regions in which the static interfacial field is significant; this distance is perhaps similar to the disordered second-order response profile. Due to the static nature of the third field, the second- and third-order signals are generated in the direction given by the sum frequency wave vector and are inseparable experimentally.[18]

Recently, a computational molecularly detailed time correlation function (TCF) method to model both the second- and third-order contributions to the SFVS signal of charged interfaces was developed. Previous theoretical studies[19−26] used a semiclassical technique to calculate quantum-corrected TCFs that describe the vibrational spectra of complex liquids and interfaces. Briefly, the approach uses classical molecular dynamics (MD) to generate trajectories for an aqueous system, while the permanent dipoles, polarizabilities, and their derivatives for each species present in the MD simulation are parametrized as a function of molecular geometry based on ab initio data. In order to construct the corresponding TCFs involving the system dipolar and polarizabilty, the induced dipoles and polarizability tensor arising from the interatomic interactions at each configuration are then calculated using a many-body, point atomic polarizability approximation (PAPA) model. This approach has been demonstrated to be an effective method for understanding the condensed-phase spectroscopy of water and other liquid interfaces and has been extended to calculate the third-order contribution to SFVS spectra at charged interfaces. Here, this extended spectroscopic model is

Special Issue: Branka M. Ladanyi Festschrift

Received: September 24, 2014
Revised: November 17, 2014

   dx.doi.org/10.1021/jp509647w | *J. Phys. Chem. B* XXXX, XXX, XXX−XXX

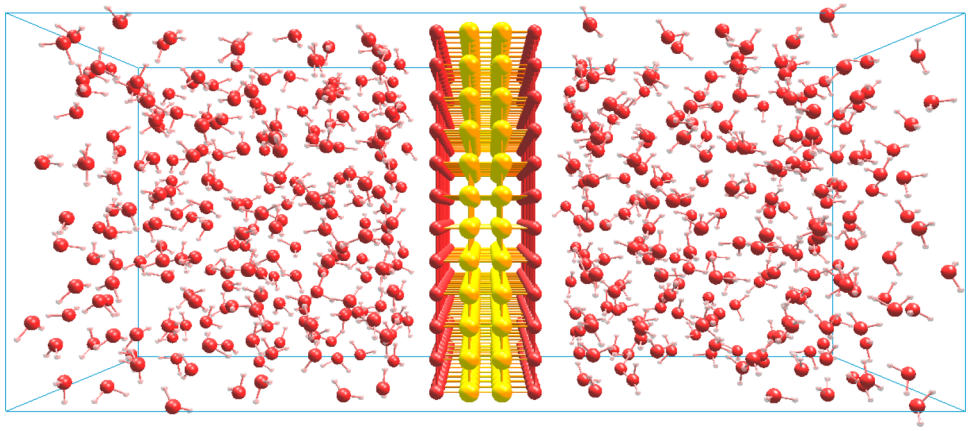

Figure 1. Charged interface snapshot. A snapshot of the abstracted and idealized aqueous interface containing 242 water molecules on each side. The silica slab is comprised of 378 oxygen atoms, shown in red, and an equal number of silicon atoms, shown in yellow.

applied to MD-generated configurations of an idealized silica/water interface in order to determine if the new model is suitable for evaluating third-order optical effects at more complex charged interfaces. The key point is that both the second- and third-order contributions to the spectra are cast as distinct TCFs that are amenable to semiclassical approximation in the fashion outlined above. Thus, the experimentally indistinguishable signal is decomposed into its distinct components.

2. MODELS AND METHODS

The system modeled during the course of this work includes a charged surface at an interface with water. Typical three-wave mixing experiments, such as SFVS, probe both the second-order, $\chi^{(2)}$, and third-order, $\chi^{(3)}$, susceptibilities in the presence of a static field created by a charged species.[27−30] The third-order polarization term can be shown to depend on an additional contribution from the electrostatic field, E_{static}, to the nonlinear polarization induced at the interface by the visible, E_{vis}, and infrared, E_{IR}, fields, and the resulting signal is given by[31]

$$P_{SFG} = P^{(2)} + P^{(3)} = \chi^{(2)} : E_{vis}E_{IR} + \chi^{(3)} \vdots E_{vis}E_{IR}E_{static} \tag{2.1}$$

Here, $P^{(2)}$ and $P^{(3)}$ denote a second- and third-order polarization, respectively. Equation 2.1 therefore implies that the measured polarization signal contains the normal second-order SFG signal represented by the first term on the right-hand side, in addition to the third-order contribution shown in the second term, which contains the presence of three fields (two incident and one static). This contribution is often not negligible,[32] and because the electrostatic field disrupts the symmetry of the system through the alignment of interfacial water molecules, it serves to extend the anisotropic interfacial region into normally centrosymmetric regions of the bulk.[33−37] This allows more molecules to contribute to the observed nonlinear polarization through both mechanisms.

Due to the wave vector of the static field being zero, the observed polarization signal, P_{SFG}, in eq 2.1 represents a combined measurement of second- and third-order processes. The wave vector of a field is proportional to its frequency, and the experimentally detected polarization signal is determined by the sum of the wave vectors, k_s, from the excitation fields.[38,39] Therefore, because the two applied fields have nonzero wave vectors, k_1 and k_2, while the static field has a wave vector of zero, the direction that the generated signal will propagate is represented by $k_s = k_1 + k_2$ and $k_s = k_1 + k_2 + 0$ for the $P^{(2)}$ and $P^{(3)}$ signals, respectively.

To investigate the third-order nonlinear polarization contribution in molecular detail computationally, it is sufficient to start with perturbation theory.[40] It has previously been shown that the 48 terms used to describe the third-order susceptibility can be simplified in terms of the real part of two different TCFs. The dominant contribution is given by cross-correlating the system's dipole and hyperpolarizability and is defined as

$$\chi^{(3),Res}_{kjiz}(\omega_{IR}) = \frac{2}{\hbar}\int_0^\infty e^{i\omega_{IR}t}\mathrm{Im}\{\langle\beta_{kzj}(t)\mu_i(0)\rangle\}\,dt \tag{2.2}$$

In eq 2.2, the imaginary part of the equation is represented by the designation Im, while β denotes the system hyperpolarizability, and z is the component perpendicular to the interface that is enhanced by the static field. The TCF in this equation is proportional to $\beta_{kzj}\mu_i$ by

$$\hbar G(t) = \langle\beta_{kzj}(t)\mu_i(0)\rangle \tag{2.3}$$

It can then be shown that analysis using detailed balance reveals that the Fourier transform of the real, $G_R(t)$, and imaginary, $G_I(t)$, parts of the TCF are analytically related by a trigonometric function factor as

$$G_I(\omega) = -\tanh(\beta\hbar\omega/2)G_R(\omega) \tag{2.4}$$

where $G_R(\omega)$ and $G_I(\omega)$ are both real. As described in previous work,[41] the classical limit can then be found, and the correlation function can be quantum-corrected to obtain an expression amenable to calculation using classical MD in conjunction with a suitable spectroscopic model and subsequent quantum correction; this constitutes the above-referenced semiclassical approach. Note, even this reasonably simple approach is not computationally trivial as the interfacial TCFs of the total system polarizability and dipole are slow to converege. Further, it is required to have an accurate model of the molecular dipoles, polarizabilities, and their derivatives simply for SFVS.

Application of the third-order contribution of TCF described (to the modeling of aqueous charged interfaces) requires the modification of the established spectroscopic model to include the calculation of the molecular and system hyperpolarizabilities. This will enable the contribution of the third-order

dx.doi.org/10.1021/jp509647w | J. Phys. Chem. B XXXX, XXX, XXX−XXX

effects resulting from the presence of a static field to be determined. To construct the spectroscopic model, point polarizabilities are assigned to each atom, such that the interactions reproduce the equilibrium gas-phase hyperpolarizability tensor.[42,43] Because the dependence on molecular geometry is included explicitly in the spectroscopic model, the hyperpolarizabilities and their derivatives were determined from fits to ab initio electronic structure calculations. Methods using appropriate basis sets have shown reliability in determining the static hyperpolarizability of gas-phase and liquid water.[44−48] Additionally, this method uses an Applequist/Thole-like model[49−53] to calculate the effective hyperpolarizability, including intrinsic and interaction effects, as sums over the products of the condensed-phase polarizability and matrices related to the dipole interaction tensor. This process is similar to the many-body polarization method that was used to calculate the polarizability in previous work. Using the Applequist/Sundberg formalism, the total effective hyperpolarizability, $\beta_{ijk}^{\mathrm{eff}}$, is given by

$$\beta_{ijk}^{\mathrm{eff}} = \sum_{n} \beta_n \frac{\alpha_{ni}^{\mathrm{eff}}}{\alpha_n} \frac{\alpha_{nj}^{\mathrm{eff}}}{\alpha_n} \frac{\alpha_{nk}^{\mathrm{eff}}}{\alpha_n} \tag{2.5}$$

where β_n denotes the intrinsic, internal molecular-geometry-dependent hyperpolarizability associated with atom n. The total effective polarizability between atom i and n is represented by $\alpha_{ni}^{\mathrm{eff}}$, and α_n is the intrinsic, internal molecular-geometry-dependent polarizability associated with atom n.

As in the previous work, MD simulations were performed using a code that uses reversible integration and extended system techniques.[54] Microcanonical MD simulations were performed on ambient H_2O with a density of 1.0 g/cm^3 and an average temperature of 298 K. To create an interface, two equally sized cubic simulation boxes of equilibrated liquid water were placed on opposite sides of an idealized flat surface along the z axis. As can be seen in Figure 1, this idealized surface was constructed as a rigid slab of double-layer charges, where one side of the slab contains a negatively charged layer followed by a positively charged layer, while the opposite side is assembled in reverse. Although this system is an idealized approximation, it is similar to glasses, such as fused quartz, and is an excellent precursor to modeling more complex water/silica interfaces. The system was allowed to equilibrate, creating two water/solid interfaces that were sufficiently far apart as to avoid strong interactions. Most results were generated from 484 water molecule simulations. Ewald summation was included in three dimensions, and the density profile of the system was monitored to verify equilibration.[55] Note, the intent is not initially to produce a totally robust model of silica or any particular charged/polar interface but to assess the expected second- and third-order contributions in terms of line shapes and sensitivities.

The MD simulations performed for this study were conducted using a rigid slab model that included intermolecular interaction potentials described by the Universal Force Field.[56] The partial charges on the silica atoms were selected to maintain charge neutrality for the system. As in previous work, the flexible simple point charge (SPC/F) water model that includes a harmonic bending potential, linear cross terms, and Morse O−H stretching potentials was used. For the purpose of modeling the spectroscopy, the partial point charges that were placed on the water atoms were chosen to reproduce the gas-phase dipole moment, and induction was included explicitly, as described above. The model system is a simplified version from a previous study[57] and is only meant to capture the polarity of the interface. The surface is chosen as a mock "silica" composed of 144 oxygen atoms and 144 silicon atoms in a simple cubic arrangement (as a first approximation) with all oxygen atoms facing outward. This arrangement is then repeated in reverse, giving an arrangement of O−Si Si−O at the center of the system to form a meaningful infinite, periodic system. On either side of the silica surface, there are 242 water molecules using the nonpolarizable flexible SPC/F model. Generally, polarizable MD models are required, but the data suggest that one can get meaningful results by only including explicitly polarization in the spectroscopic calculation. The atoms of the silica surface are held rigid with a Si−O radius of 1.61 Å in accordance with experiment and given charges of +0.6 and −0.6 for silicon and oxygen, respectively, for two model calculations. This balances the overall charge on the system and roughly approximates a neutral pH level. A second model was generated with charges of +2.0 assigned to silcon and −2.0 assigned to oxygen atoms in order to approximate a highly basic system.[58−60]

3. RESULTS AND DISCUSSION

Figure 2 shows the theoretical description of the SFVS spectrum derived using the third-order TCF method for the entire water vibrational spectrum of the idealized silica/water interface in the SSP polarization condition. As expected, there is a now dominate feature in the O−H stretching region. The resonance seen at around 1800 cm^{-1} is somewhat intense (as compared to the previous interfacial spectra) and is due to bending motion of bulk water molecules near the interface. This increase in intensity, compared to previous studies of second-order SFVS at neat water/vapor interfaces, suggests that the interface has been extended farther into the bulk (i.e., disrupting the symmetry) or that the dynamics near the interface are affected by the presence of the charged surface, thus allowing a greater contribution to the SFVS spectra from this typically bulk-like behavior.

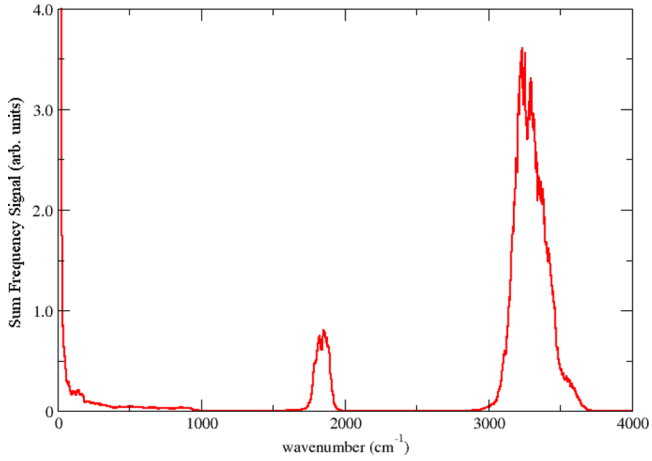

Figure 2. Third-order SFVS spectrum for the silica/water interface. SFVS spectrum using the third-order TCF method in the SSP polarization condition for the idealized silica/water interface for the entire water vibrational spectrum.

Figure 3 presents the theoretical third-order TCF SFVS spectrum in the O−H stretching region for the SSP polarization condition. Here, two peaks in the area between 3100 and 3500 cm^{-1} are clearly identifiable. The first peak at

dx.doi.org/10.1021/jp509647w | J. Phys. Chem. B XXXX, XXX, XXX−XXX

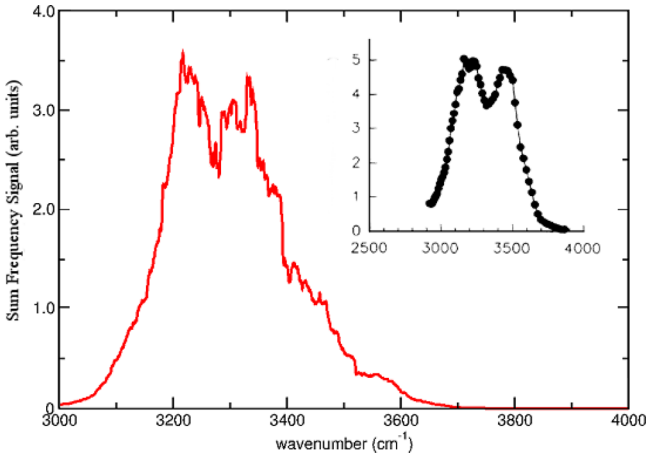

Figure 3. Third-order SFVS spectrum for the O−H stretching region of the silica/water interface. The third-order TCF SFVS spectrum for the idealized silica/water interface in the O−H stretching region for the SSP polarization condition calculated from theory (solid red line). The inset is experimental data[58] for the same polarization geometry.

approximately 3200 cm^{-1} has been attributed to ice-like ordering of the water molecules near the interface, while the second peak that occurs at around 3400 cm^{-1} has been described as more liquid-like and is similar to the peak seen in the donor O−H region of the water/vapor spectrum, although these interpretations are a subject of much debate. The free O−H peak that normally occurs at around 3700 cm^{-1} is clearly suppressed, which is indicative of a distorted ice-like hydrogen-bonding network formed by the water molecules at this surface.[61] The inset of Figure 3 displays experimental data for the O−H stretching region of a fused quartz/water interface taken in the same polarization geometry. The theoretical and experimental line shapes are surprisingly similar.

For comparison with the third-order model, Figure 4 shows the spectrum for the same system and polarization geometry in the O−H stretching region using the established second-order TCF expression. Using this method, the peaks appear less well defined, and the signal intensity is reduced by an order of magnitude. The detailed reason for the poor averaging of the second-order signal is unclear, and the results are incredibly slow in converging. While more refinement of the model is needed, this comparison suggests that the third-order contribution does play an important role in determining the spectra of a charged interface.

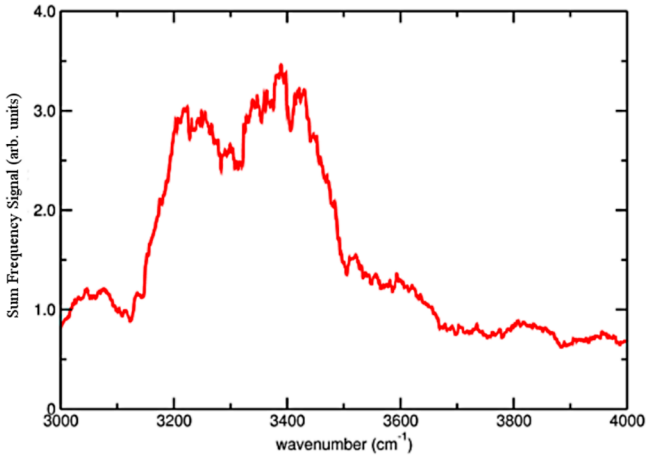

Figure 4. Second-order SFVS spectrum for the O−H stretching region of the silica/water interface. SFVS spectrum for the idealized silica/water interface in the O−H stretching region for the SSP polarization condition using the second-order TCF model.

Additional simulations were carried out using a model charged interface with higher pH values. The resulting third-order SFVS spectrum of the O−H stretch from calculation is shown in Figure 5, along with the experimental second-order

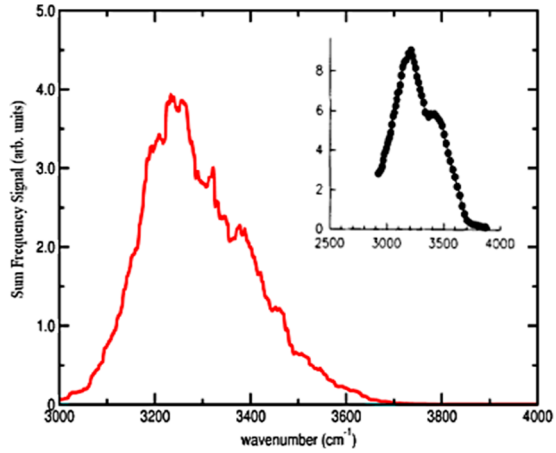

Figure 5. Third-order SFVS spectrum of the silica/water interface at high pH. The third-order TCF SFVS spectrum for the idealized highly basic silica/water interface in the O−H stretching region for the SSP polarization condition calculated from theory (solid red line). The inset is experimental data[58] for the same polarization geometry.

SFVS signal from silica at the corresponding basic pH value. When considering that the spectrum in Figure 3 is characteristic of neutral pH, the similarity between simulation and experiment is remarkable and strongly suggests that the third-order signal closely mimics the second-order spectrum even though it arises from a distinct physical process originating from the hyperpolarizabilty derivative with differing interface specificity.[62] The interfacial waters are also seen to be more highly ordered at the higher charged interface and can be quantitatively examined as a function of field strength. Further, the results shown in Figure 5 strongly suggest that the signal associated with water ordering at charged interfaces has universal characteristics; even this simple model, lacking the atomistic detail of real silica, closely reproduces observed silica spectra over a broad pH range. This also implies a largely field-dependent ordering of water at such boundaries.

4. CONCLUSIONS

Theoretical approximations to the interface-specific SFVS spectrum of O−H stretching at the water/silica interface have been calculated based on MD simulations of water at an idealized silica slab surface. Spectra are constructed using newly developed static-field-enhanced TCF methods. This approach leads to a signal in the SSP polarization geometry that is comparable with experimental measurements. SFVS is an inherently challenging second-order optical technique, and studies on water interfaces concentrate on the line shape associated with the intense O−H stretching resonance that is perturbed by the inhomogeneous environment. The presence of a static field associated with the charged species can produce an apparent ice-like ordering of water molecules in the OH

dx.doi.org/10.1021/jp509647w | J. Phys. Chem. B XXXX, XXX, XXX−XXX

stretching region at the interface, which corresponds to published experimental data at an interface with α-quartz. The complexity of the broad structured SFVS signal can be attributed to O−H stretching motions facing toward the bulk or silica surface environments that are characteristic of the interface. Achieving agreement with experimental measurements engenders confidence in the MD and spectroscopic models used to produce the theoretical spectrum and suggests that theory can play a crucial role in interpreting SFVS spectra at more complex interfaces. Further, it is remarkable that the simple model system appears to contain the essential physics of the problem; the polar nature of the interface is more important than the detailed geometry and chemical structure. In sum, even the simple model system strongly suggests that third-order SFVS effects can produce signals with shapes that are at least very similar to second-order spectra or that experiments are measuring some combination of the two effects. This is just the kind of problem that the theoretical spectroscopic methods developed and applied here are ideally suited to resolve. With the emergence of SFVS spectroscopy as an analytic technique in many diverse fields, these studies represent a timely attempt to clarify the specificity of SFVS spectroscopy at charged/polar interfaces.

Additional investigation and refinement of this model is clearly required, but the initial results are promising and build on previous success in understanding the complex structure and dynamics of aqueous interfaces. Future work may determine the level of importance of third-order signals and whether ordering of the interfacial water structure contributes to an enhanced second-order signal.

AUTHOR INFORMATION

Corresponding Author

*E-mail: bspace@mail.usf.edu.

Notes

The authors declare no competing financial interest.

ACKNOWLEDGMENTS

The authors would like to acknowledge the National Science Foundation and the Space Foundation for Basic and Applied Research for support of this research work. The simulations were carried out using resources and services provided by Research Computing at the University of South Florida.

REFERENCES

(1) Iler, R. K. *The Chemistry of Silica*; Wiley: New York, 1979.
(2) Legrand, A. P. *The Surface Properties of Silicas*; Wiley: New York, 1998.
(3) Al-Abadleh, H. A.; Mifflin, A. L.; Musorrafiti, M. J.; Geiger, F. M. Kinetic studies of chromium (VI) binding to carboxylic acid- and methyl ester-functionalized silica/water interfaces important in geochemistry. *J. Phys. Chem. B* **2005**, *109* (35), 16852−16859.
(4) Evangelou, V. *Environmental Soil and Water Chemistry*; Wiley: New York, 1996.
(5) Langmuir, D. *Aqueous Environmental Geochemistry*; Prentice Hall: Englewood Cliffs, NJ, 1997.
(6) Sakong, S.; Kratzer, P.; Wall, S.; Kalus, A.; Horn-von Hoegen, M. Mode conversion and long-lived vibrational modes in lead monolayers on silicon(111) after femtosecond laser excitation: A molecular dynamics simulation. *Phys. Rev. B* **2013**, *88* (11), 115419.
(7) Lopes, P. E.; Murashov, V.; Tazi, M.; Demchuk, E.; MacKerell, A. D. Development of an empirical force field for silica. Application to the quartz−water interface. *J. Phys. Chem. B* **2006**, *110* (6), 2782−2792.
(8) Sulpizi, M.; Gaigeot, M. P.; Sprik, M. The silica−water interface: How the silanols determine the surface acidity and modulate the water properties. *J. Chem. Theory Comput.* **2012**, *8* (3), 1037−1047.
(9) Hassanali, A. A.; Singer, S. J. Model for the water−amorphous silica interface: The undissociated surface. *J. Phys. Chem. B* **2007**, *111* (38), 11181−11193.
(10) Robertson, E. J.; Richmond, G. L. Chunks of Charge: Effects at Play in the Assembly of Macromolecules at Fluid Surfaces. *Langmuir* **2013**, *29* (35), 10980−10989.
(11) Morita, A.; Hynes, J. T. A theoretical analysis of the sum frequency generation spectrum of the water surface. II. Time-dependent approach. *J. Phys. Chem. B* **2002**, *106* (3), 673−685.
(12) Wei, X.; Shen, Y. R. Motional effect in surface sum-frequency vibrational spectroscopy. *Phys. Rev. Lett.* **2001**, *86* (21), 4799.
(13) Lin, C. K.; Yang, L.; Hayashi, M.; Zhu, C. Y.; Fujimura, Y.; Shen, Y. R.; Lin, S. H. Theory and Applications of Sum-Frequency Generations. *J. Chin. Chem. Soc.* **2014**, *61* (1), 77−92.
(14) Eisenthal, K. B. Liquid interfaces probed by second-harmonic and sum-frequency spectroscopy. *Chem. Rev.* **1996**, *96* (4), 1343−1360.
(15) Robertson, E. J.; Beaman, D. K.; Richmond, G. L. Designated Drivers: The Differing Roles of Divalent Metal Ions in Surfactant Adsorption at the Oil−Water Interface. *Langmuir* **2013**, *29* (50), 15511−15520.
(16) Geissler, P. L. Water Interfaces, Solvation, and Spectroscopy. *Annu. Rev. Phys. Chem.* **2013**, *64*, 317−337.
(17) Lu, X.; Clarke, M. L.; Li, D.; Wang, X.; Xue, G.; Chen, Z. A sum frequency generation vibrational study of the interference effect in poly(*n*-butyl methacrylate) thin films sandwiched between silica and water. *J. Phys. Chem. C* **2011**, *115* (28), 13759−13767.
(18) Sung, W.; Kim, D.; Shen, Y. R. Sum-frequency vibrational spectroscopic studies of Langmuir monolayers. *Curr. Appl. Phys.* **2013**, *13* (4), 619−632.
(19) Perry, A.; Ahlborn, H.; Space, B.; Moore, P. B. A combined time correlation function and instantaneous normal mode study of the sum frequency generation spectroscopy of the water/vapor interface. *J. Chem. Phys.* **2003**, *118* (18), 8411−8419.
(20) Perry, A.; Neipert, C.; Ridley, C.; Space, B.; Moore, P. B. Identification of a wagging vibrational mode of water molecules at the water/vapor interface. *Phys. Rev. E* **2005**, *71* (5), 050601.
(21) Perry, A.; Neipert, C.; Kasprzyk, C. R.; Green, T.; Space, B.; Moore, P. B. A theoretical description of the polarization dependence of the sum frequency generation spectroscopy of the water/vapor interface. *J. Chem. Phys.* **2005**, *123* (14), 144705.
(22) Green, A. J.; Perry, A.; Moore, P. B.; Space, B. A theoretical study of the sum frequency vibrational spectroscopy of the carbon tetrachloride/water interface. *J. Phys.: Condens. Matter* **2012**, *24* (12), 124108.
(23) Ahlborn, H.; Space, B.; Moore, P. B. The effect of isotopic substitution and detailed balance on the infrared spectroscopy of water: A combined time correlation function and instantaneous normal mode analysis. *J. Chem. Phys.* **2000**, *112* (18), 8083−8088.
(24) Ji, X.; Ahlborn, H.; Space, B.; Moore, P. B.; Zhou, Y.; Constantine, S.; Ziegler, L. D. A combined instantaneous normal mode and time correlation function description of the optical Kerr effect and Raman spectroscopy of liquid CS_2. *J. Chem. Phys.* **2000**, *112* (9), 4186−4192.
(25) Ahlborn, H.; Ji, X.; Space, B.; Moore, P. B. A combined instantaneous normal mode and time correlation function description of the infrared vibrational spectrum of ambient water. *J. Chem. Phys.* **1999**, *111* (23), 10622−10632.
(26) Mankoo, P. K.; Keyes, T. Classical molecular electrostatics: Recognition of ligands in proteins and the vibrational stark effect. *J. Phys. Chem. B* **2006**, *110* (49), 25074−25079.
(27) Ostroverkhov, V.; Waychunas, G. A.; Shen, Y. R. New information on water interfacial structure revealed by phase-sensitive surface spectroscopy. *Phys. Rev. Lett.* **2005**, *94* (4), 0461021.

(28) Gragson, D. E.; McCarty, B. M.; Richmond, G. L. Surfactant/water interactions at the air/water interface probed by vibrational sum frequency generation. *J. Phys. Chem.* **1996**, *100* (34), 14272−14275.
(29) Kim, J.; Cremer, P. S. IR−visible SFG investigations of interfacial water structure upon polyelectrolyte adsorption at the solid/liquid interface. *J. Am. Chem. Soc.* **2000**, *122* (49), 12371−12372.
(30) Puibasset, J.; Pellenq, R. J. A grand canonical Monte Carlo simulation study of water adsorption on Vycor-like hydrophilic mesoporous silica at different temperatures. *J. Phys.: Condens. Matter* **2004**, *16* (45), S5329.
(31) Gragson, D. E.; Richmond, G. L. Probing the structure of water molecules at an oil/water interface in the presence of a charged soluble surfactant through isotopic dilution studies. *J. Phys. Chem. B* **1998**, *102* (3), 569−576.
(32) Bordenyuk, A. N.; Benderskii, A. V. Spectrally- and time-resolved vibrational surface spectroscopy: Ultrafast hydrogen-bonding dynamics at D_2O/CaF_2 interface. *J. Chem. Phys.* **2005**, *122* (13), 134713.
(33) Du, Q.; Superfine, R.; Freysz, E.; Shen, Y. R. Vibrational spectroscopy of water at the vapor/water interface. *Phys. Rev. Lett.* **1993**, *70* (15), 2313.
(34) Gragson, D. E.; Richmond, G. L. Potential dependent alignment and hydrogen bonding of water molecules at charged air/water and CCl_4/water interfaces. *J. Am. Chem. Soc.* **1998**, *120* (2), 366−375.
(35) Gragson, D. E.; McCarty, B. M.; Richmond, G. L. Ordering of interfacial water molecules at the charged air/water interface observed by vibrational sum frequency generation. *J. Am. Chem. Soc.* **1997**, *119* (26), 6144−6152.
(36) Held, H.; Lvovsky, A. I.; Wei, X.; Shen, Y. R. Bulk contribution from isotropic media in surface sum-frequency generation. *Phys. Rev. B* **2002**, *66* (20), 205110.
(37) Shultz, M. J.; Schnitzer, C.; Simonelli, D.; Baldelli, S. Sum frequency generation spectroscopy of the aqueous interface: ionic and soluble molecular solutions. *Int. Rev. Phys. Chem.* **2000**, *19* (1), 123−153.
(38) Shen, Y. R. *Principles of Nonlinear Optics*; Wiley: New York, 1984.
(39) Boyd, R. W. *Nonlinear Opt.*; Academic Press: London, 2003.
(40) Orr, B. J.; Ward, J. F. Perturbation theory of the non-linear optical polarization of an isolated system. *Mol. Phys.* **1971**, *20* (3), 513−526.
(41) DeVane, R.; Space, B.; Perry, A.; Neipert, C.; Ridley, C.; Keyes, T. A time correlation function theory of two-dimensional infrared spectroscopy with applications to liquid water. *J. Chem. Phys.* **2004**, *121* (8), 3688−3701.
(42) Jensen, L. Modelling of Optical Response Properties: Application to Nanostructures. Ph.D. Thesis, University of Gorningen, The Netherlands, 2004.
(43) Sundberg, K. R. A group−dipole interaction model of the molecular polarizability and the molecular first and second hyperpolarizabilities. *J. Chem. Phys.* **1977**, *66* (1), 114−118.
(44) Gritsenko, O. V.; Schipper, P. R. T.; Baerends, E. J. Approximation of the exchange−correlation Kohn−Sham potential with a statistical average of different orbital model potentials. *Chem. Phys. Lett.* **1999**, *302* (3), 199−207.
(45) Gritsenko, O. V.; Schipper, P. R. T.; Baerends, E. J. Ensuring proper short-range and asymptotic behavior of the exchange−correlation Kohn−Sham potential by modeling with a statistical average of different orbital model potentials. *Int. J. Quantum Chem.* **2000**, *76* (3), 407−419.
(46) Schipper, P. R. T.; Gritsenko, O. V.; van Gisbergen, S. J.; Baerends, E. J. Molecular calculations of excitation energies and (hyper)polarizabilities with a statistical average of orbital model exchange−correlation potentials. *J. Chem. Phys.* **2000**, *112* (3), 1344−1352.
(47) Gubskaya, A. V.; Kusalik, P. G. The multipole polarizabilities and hyperpolarizabilities of the water molecule in liquid state: an ab initio study. *Mol. Phys.* **2001**, *99* (13), 1107−1120.
(48) Gubskaya, A. V.; Kusalik, P. G. A mean-field approach for the determination of the polarizabilities for the water molecule in liquid state. *J. Comput. Methods Sci. Eng.* **2004**, *4* (4), 641−664.
(49) Thole, B. T. Molecular polarizabilities calculated with a modified dipole interaction. *Chem. Phys.* **1981**, *59* (3), 341−350.
(50) Ladanyi, B. M.; Keyes, T.; Tildesley, D. J.; Streett, W. B. Structure and equilibrium optical properties of liquid CS_2. *Mol. Phys.* **1980**, *39* (3), 645−659.
(51) Geiger, L. C.; Ladanyi, B. M.; Chapin, M. E. A comparison of models for depolarized light scattering in supercritical CO_2. *J. Chem. Phys.* **1990**, *93* (7), 4533−4542.
(52) Bernardo, D. N.; Ding, Y.; Krogh-Jespersen, K.; Levy, R. M. An anisotropic polarizable water model: incorporation of all-atom polarizabilities into molecular mechanics force fields. *J. Phys. Chem.* **1994**, *98* (15), 4180−4187.
(53) Burnham, C. J.; Li, J.; Xantheas, S. S.; Leslie, M. The parametrization of a Thole-type all-atom polarizable water model from first principles and its application to the study of water clusters (n = 2−21) and the phonon spectrum of ice Ih. *J. Chem. Phys.* **1999**, *110* (9), 4566−4581.
(54) Tuckerman, M.; Berne, B. J.; Martyna, G. J. Reversible multiple time scale molecular dynamics. *J. Chem. Phys.* **1992**, *97* (3), 1990−2001.
(55) Taylor, R. S.; Dang, L. X.; Garrett, B. C. Molecular dynamics simulations of the liquid/vapor interface of SPC/E water. *J. Phys. Chem.* **1996**, *100* (28), 11720−11725.
(56) Rappe, A. K.; Casewit, C. J.; Colwell, K. S.; Goddard, W. A., III; Skiff, W. M. UFF, a full periodic table force field for molecular mechanics and molecular dynamics simulations. *J. Am. Chem. Soc.* **1992**, *114* (25), 10024−10035.
(57) Koudriachova, M. V.; Beckers, J. V. L; De Leeuw, S. W. Computer simulation of the quartz surface: a combined ab initio and empirical potential approach. *Comput. Mater. Sci.* **2001**, *20* (3), 381−386.
(58) Du, Q.; Freysz, E.; Shen, Y. R. Vibrational spectra of water molecules at quartz/water interfaces. *Phys. Rev. Lett.* **1994**, *72* (2), 238.
(59) Ostroverkhov, V.; Waychunas, G. A.; Shen, Y. R. Vibrational spectra of water at water/α-quartz(0001) interface. *Chem. Phys. Lett.* **2004**, *386* (1), 144−148.
(60) Azam, M. S.; Weeraman, C. N.; Gibbs-Davis, J. M. Specific Cation Effects on the Bimodal Acid−Base Behavior of the Silica/Water Interface. *J. Phys. Chem. Lett.* **2012**, *3* (10), 1269−1274.
(61) Shen, Y. R.; Ostroverkhov, V. Sum-frequency vibrational spectroscopy on water interfaces: Polar orientation of water molecules at interfaces. *Chem. Rev.* **2006**, *106* (4), 1140−1154.
(62) Isaienko, O.; Nihonyanagi, S.; Sil, D.; Borguet, E. Observation of the Bending Mode of Interfacial Water at Silica Surfaces by Near-Infrared Vibrational Sum-Frequency Generation Spectroscopy of the [Stretch + Bend] Combination Bands. *J. Phys. Chem. Lett.* **2013**, *4* (3), 531−535.